Measurements of production cross sections of the Higgs boson in the four-lepton final state in proton–proton collisions at 13 TeV with the CMS detector

Qianying GUO

(Beihang University && Institute of High Energy Physics, Beijing)

On behalf of CMS collaboration

The 7th China LHC Physics Workshop (CLHCP2021)

Introduction

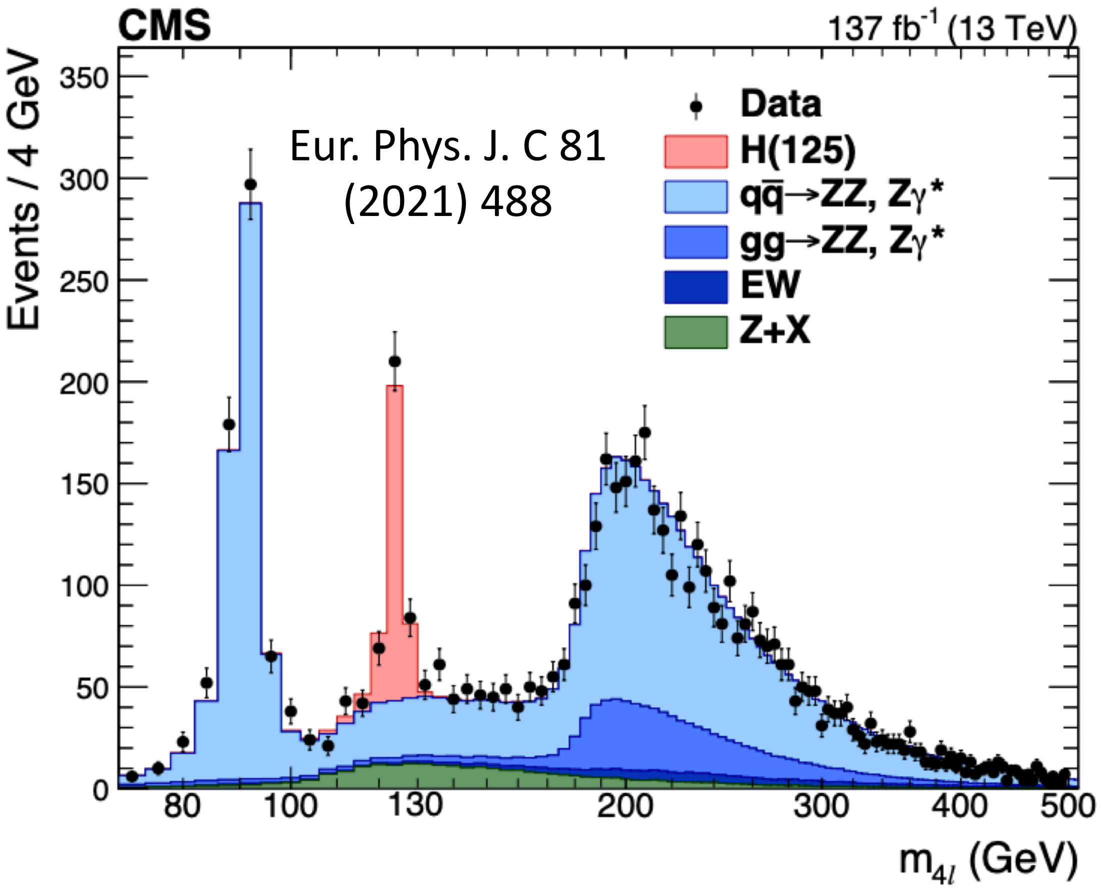

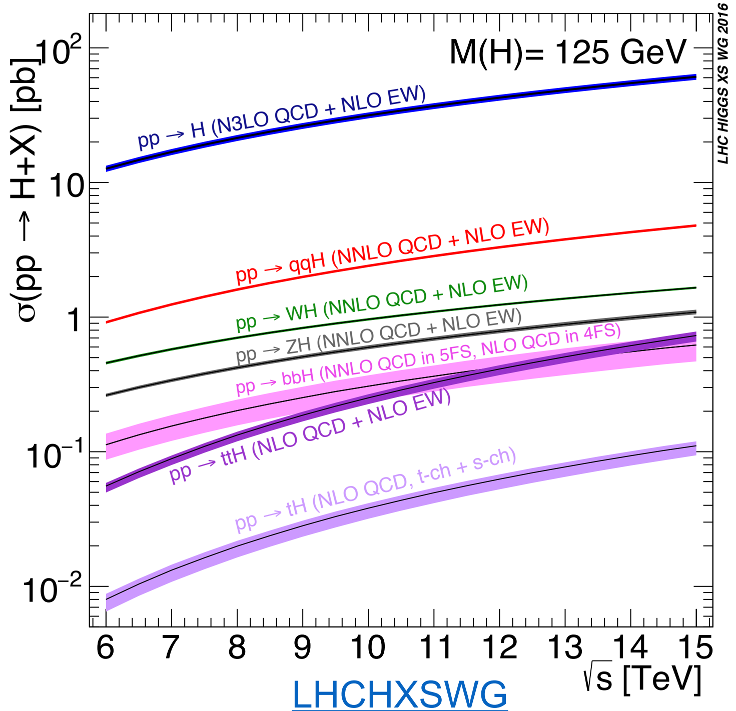

LHCHXSWG

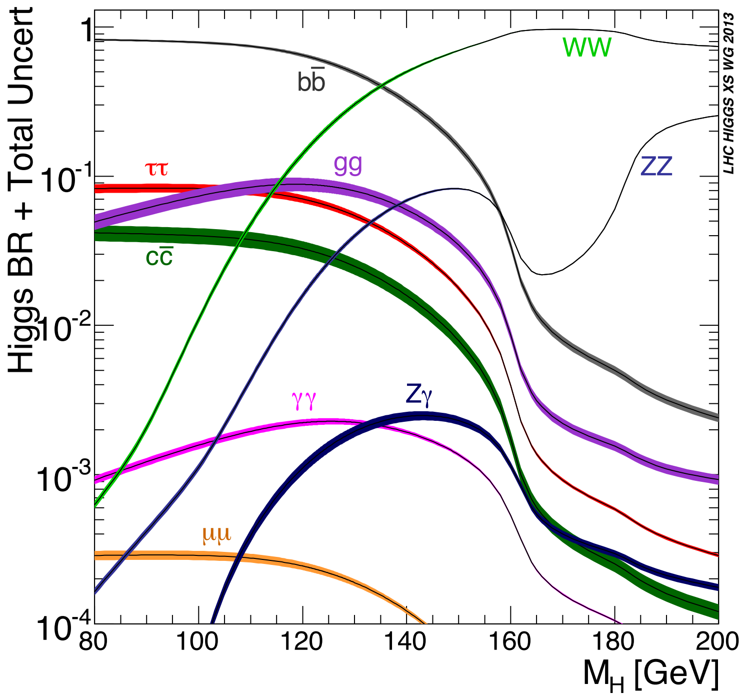

- 4l channel is one of the most important channel for property measurement of Higgs boson
  - A large signal-to-background ratio
  - Complete reconstruction of final state decay products
  - Excellent lepton momentum reconstruction

Analysis Strategy-- Event reconstruction and selections

- Loose e (μ) passing selections $P_T > 7(5)$GeV; $|\eta| < 2.5(2.4)$; vertex cut $d_{xy} < 0.5\ cm$; $d_z < 1\ cm$;$SIP_{3D} < 3$; BDT Selections (RelPFIso($\Delta R = 0.3) < 0.35$);
- Z candidate
  - Any OS-SF pair that satisfy $12 < m_{ll(\gamma)} < 120$ GeV
- Build all possible ZZ candidates defined as pairs of non-overlapping Z candidate; define Z_1 candidate with $m_{ll(\gamma)}$ closest to the POG m(Z) mass
  - $m_{Z1} > 40$ GeV; $P_T(l1) > 20$ GeV; $P_T(l2) > 10$ GeV
  - $\Delta R > 0.02$ between each of the four leptons
  - $m_{ll} > 4$ GeV for OS pairs (regardless of flavour)
  - Reject 4μ and 4e candidates where the alternative pair Z_aZ_b satisfies $|m_{Z_a} - m_Z| < |m_{Z_1} - m_Z|$ and $m_{Z_b} < 12$ GeV
  - $m_{4l} > 70$ GeV
- If more than one ZZ candidate is left, choose the one of highest $\mathcal{D}_{bkg}^{kin}$.
- If $\mathcal{D}_{bkg}^{kin}$ is the same, take the one with Z_1 mass closest to m_Z.

Observables

- Two observables used: m_{4l}; kd
- Three different kd discriminant applied.
  - Discriminant sensitive to gg/$q\bar{q} \rightarrow 4l$ kinematics
  - Dedicated production-dependent $\mathcal{D}_{\rm kgd}$ discriminants used in VBF-2jet tagged and hadronic VH tagged categories
  - Four discriminants calculated are used to enhance the purity of event categories

$$\mathcal{D}^{\rm kin}_{\rm bkg} = \left[1 + \frac{\mathcal{P}^{q\bar{q}}_{\rm bkg}(\vec{\Omega}^{\rm H\to4\ell}|m_{4\ell})}{\mathcal{P}^{\rm gg}_{\rm sig}(\vec{\Omega}^{\rm H\to4\ell}|m_{4\ell})}\right]^{-1} \quad (1)$$

$$\mathcal{D}^{\rm VBF+dec}_{\rm bkg} = \left[1 + \frac{c^{\rm VBF}(m_{4\ell})[\mathcal{P}^{\rm EW}_{\rm bkg}(\vec{\Omega}^{\rm H+jj}|m_{4\ell}) + \mathcal{P}^{\rm QCD}_{\rm bkg}(\vec{\Omega}^{\rm H+jj}|m_{4\ell})]}{\mathcal{P}^{\rm EW}_{\rm sig}(\vec{\Omega}^{\rm H+jj}|m_{4\ell})}\right]^{-1}$$

$$\mathcal{D}^{\rm VH+dec}_{\rm bkg} = \left[1 + \frac{c^{\rm VH}(m_{4\ell})[\mathcal{P}^{\rm EW}_{\rm bkg}(\vec{\Omega}^{\rm H+jj}|m_{4\ell}) + \mathcal{P}^{\rm QCD}_{\rm bkg}(\vec{\Omega}^{\rm H+jj}|m_{4\ell})]}{\mathcal{P}^{\rm EW}_{\rm sig}(\vec{\Omega}^{\rm H+jj}|m_{4\ell})}\right]^{-1} \quad (2)$$

$$\mathcal{D}^{\rm VBF}_{\rm 2jet} = \left[1 + \frac{\mathcal{P}_{\rm Hjj}(\vec{\Omega}^{\rm H+jj}|m_{4\ell})}{\mathcal{P}_{\rm VBF}(\vec{\Omega}^{\rm H+jj}|m_{4\ell})}\right]^{-1}$$

$$\mathcal{D}^{\rm WH}_{\rm 2jet} = \left[1 + \frac{\mathcal{P}_{\rm Hjj}(\vec{\Omega}^{\rm H+jj}|m_{4\ell})}{\mathcal{P}_{\rm WH}(\vec{\Omega}^{\rm H+jj}|m_{4\ell})}\right]^{-1}$$

$$\mathcal{D}^{\rm VBF}_{\rm 1jet} = \left[1 + \frac{\mathcal{P}_{\rm Hj}(\vec{\Omega}^{\rm H+j}|m_{4\ell})}{\int d\eta^{j}\mathcal{P}_{\rm VBF}(\vec{\Omega}^{\rm H+jj}|m_{4\ell})}\right]^{-1}$$

$$\mathcal{D}^{\rm ZH}_{\rm 2jet} = \left[1 + \frac{\mathcal{P}_{\rm Hjj}(\vec{\Omega}^{\rm H+jj}|m_{4\ell})}{\mathcal{P}_{\rm ZH}(\vec{\Omega}^{\rm H+jj}|m_{4\ell})}\right]^{-1} \quad (3)$$

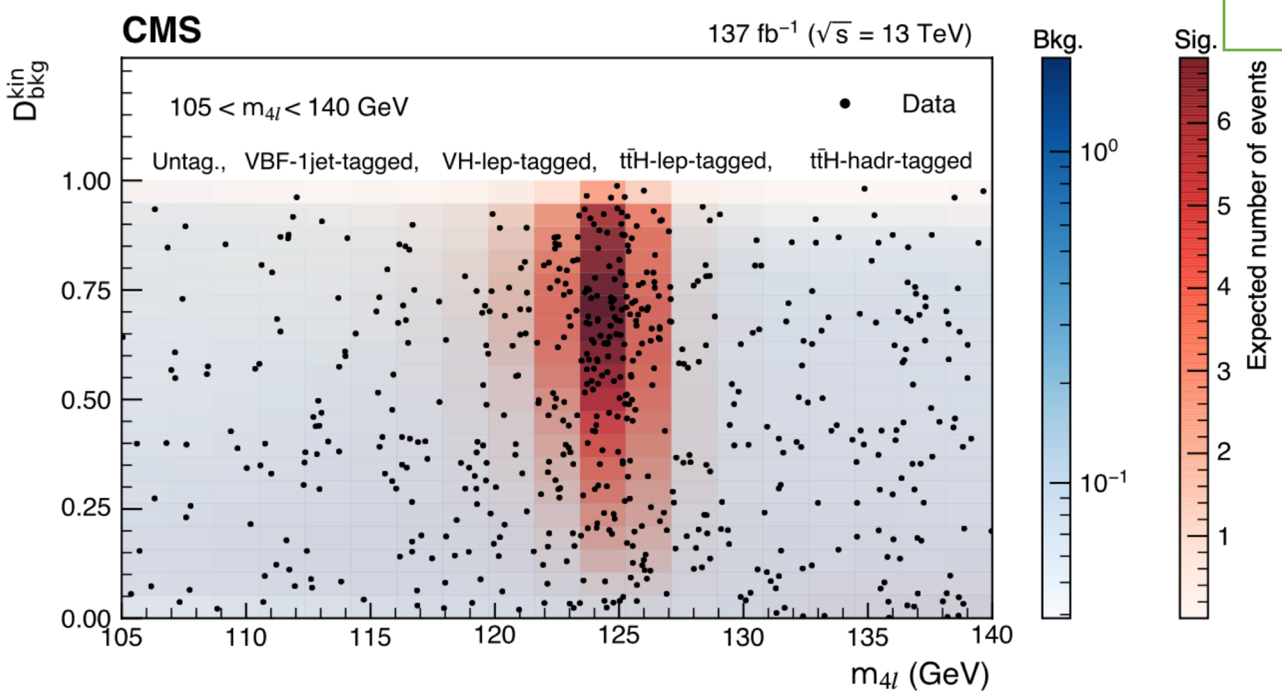

Eur. Phys. J. C 81 (2021) 488

STXS Production Bins-- STXS1.2 bins

- The primary goals of the STXS framework are to maximize the sensitivity of the measurements while at the same time to minimize their dependence on the theory predictions.
- The events are further binned within ggH, VBF, and VH in order to study deeper structure within each production mechanisms. (10+6+2+1)

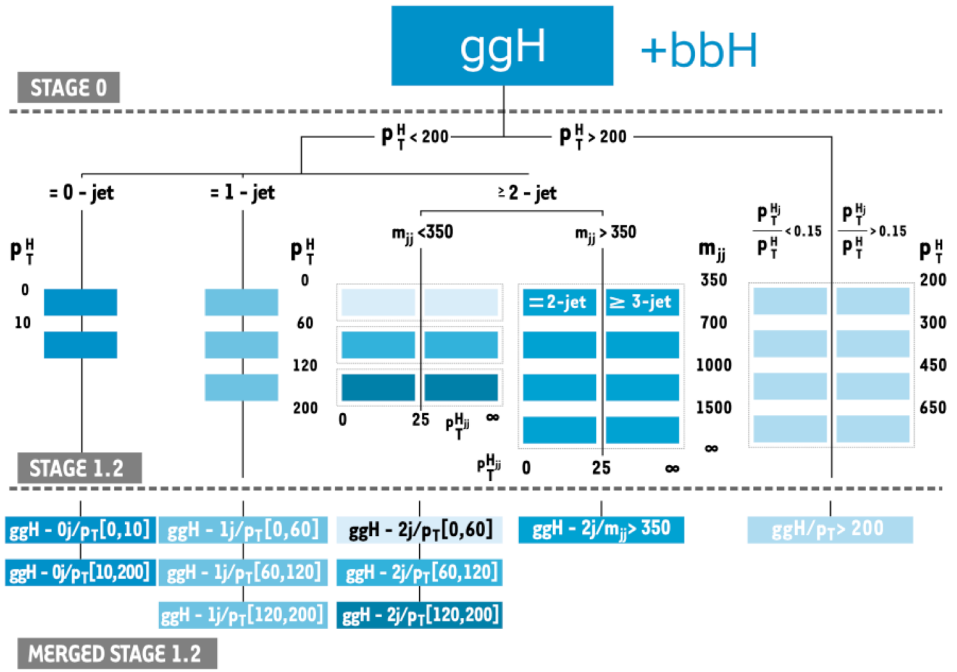

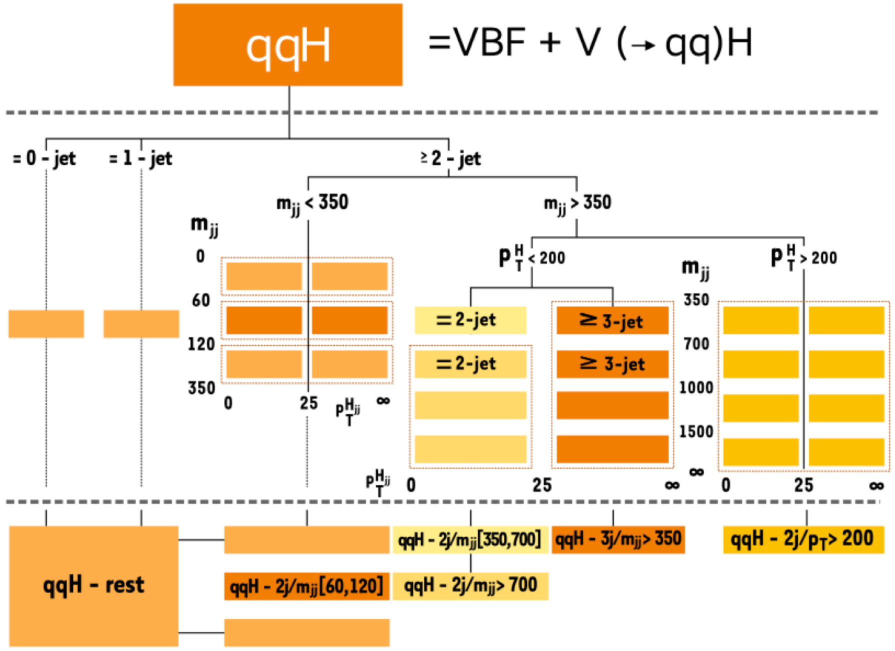

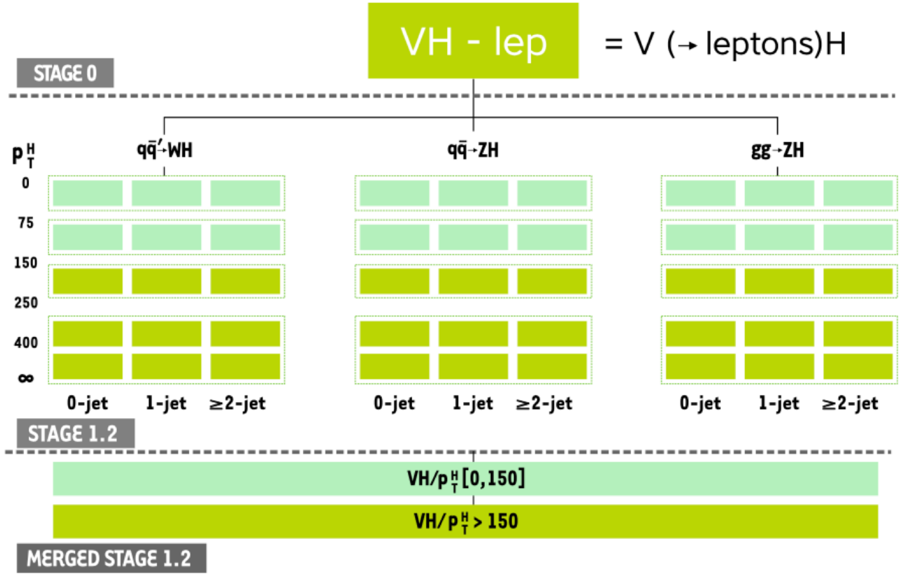

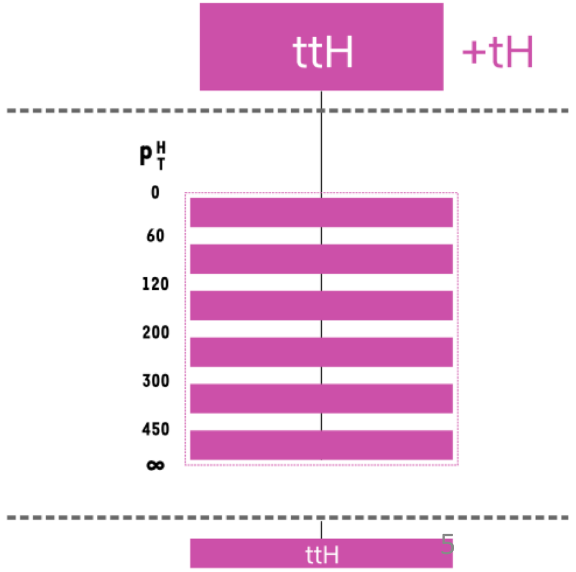

Reconstructed Event categorization – Stage0

- Selected events are classified into seven exclusive categories to improve the sensitivity to the Higgs boson production mechanisms.

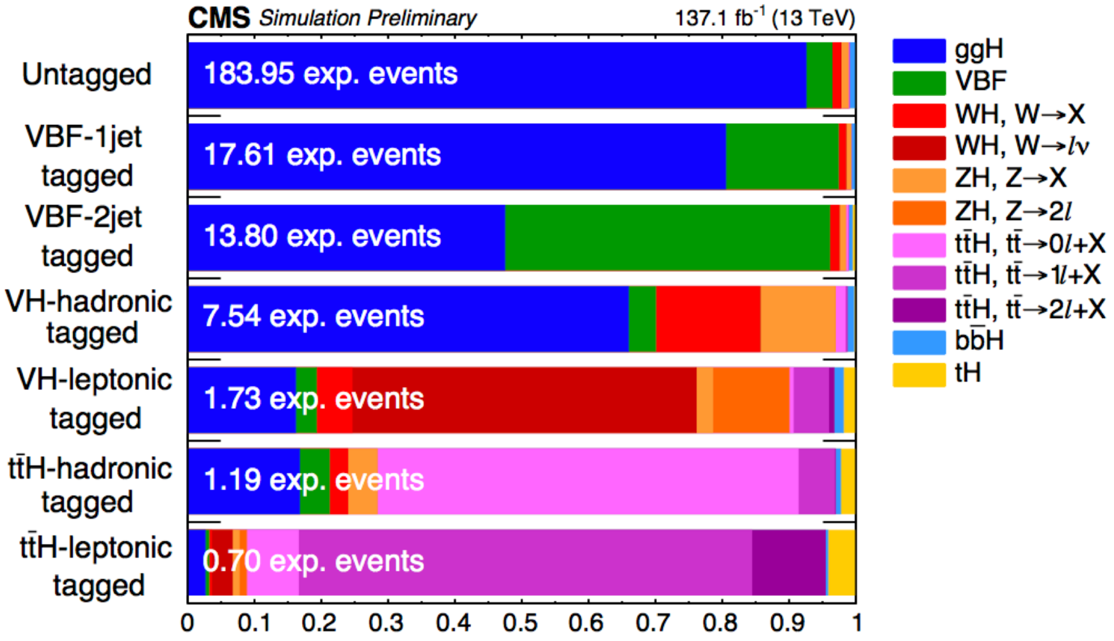

CMS PAS HIG-19-001

- **VBF-2jet-tagged category** requires exactly 4 leptons. In addition there must be either 2 or 3 jets of which at most 1 is b-tagged, or at least 4 jets and no b-tagged jets. Finally, $\mathcal{D}_{2\text{jet}} > 0.5$ is required.
- **VH-hadronic-tagged category** requires exactly 4 leptons. In addition there must be 2 or 3 jets, or at least 4 jets and no b-tagged jets. Finally, $\mathcal{D}_{\text{VH}} > 0.5$ is required.
- **VH-leptonic-tagged category** requires no more than 3 jets and no b-tagged jets in the event, and exactly 1 additional lepton or 1 additional pair of opposite sign same flavor leptons. This category also includes events with no jets and at least 1 additional lepton.
- **tt̄H-hadronic-tagged category** requires at least 4 jets of which at least 1 is b-tagged and no additional leptons.
- **tt̄H-leptonic-tagged category** requires at least 1 additional lepton in the event.
- **VBF-1jet-tagged category** requires exactly 4 leptons, exactly 1 jet and $\mathcal{D}_{1\text{jet}} > 0.7$.
- **Untagged category** consists of the remaining events.

Reconstructed Event categorization – Stage1.2

- Events are Further subdivided in the second step to closely match the merged stage 1.2 production bins by exploiting additional variables.

Reconstructed event category	1[st] categorization step	Number of jets	Kinematical requirements (GeV)	Targeted production bin
Untagged-0j-$p_T^{4\ell}[0,10]$	Untagged	0	$0 < p_T^{4\ell} < 10$	ggH-0j/$p_T[0,10]$
Untagged-0j-$p_T^{4\ell}[10,200]$	Untagged	0	$10 < p_T^{4\ell} < 200$	ggH-0j/$p_T[10,200]$
Untagged-1j-$p_T^{4\ell}[0,60]$	Untagged	1	$0 < p_T^{4\ell} < 60$	ggH-1j/$p_T[0,60]$
Untagged-1j-$p_T^{4\ell}[60,120]$	Untagged	1	$60 < p_T^{4\ell} < 120$	ggH-1j/$p_T[60,120]$
Untagged-1j-$p_T^{4\ell}[120,200]$	Untagged	1	$120 < p_T^{4\ell} < 200$	ggH-1j/$p_T[120,200]$
Untagged-2j-$p_T^{4\ell}[0,60]$	Untagged	2	$0 < p_T^{4\ell} < 60$, $m_{jj} < 350$	ggH-2j/$p_T[0,60]$
Untagged-2j-$p_T^{4\ell}[60,120]$	Untagged	2	$60 < p_T^{4\ell} < 120$, $m_{jj} < 350$	ggH-2j/$p_T[60,120]$
Untagged-2j-$p_T^{4\ell}[120,200]$	Untagged	2	$120 < p_T^{4\ell} < 200$, $m_{jj} < 350$	ggH-2j/$p_T[120,200]$
Untagged-$p_T^{4\ell} > 200$	Untagged	—	$p_T^{4\ell} > 200$	ggH/$p_T > 200$
Untagged-2j-$m_{jj} > 350$	Untagged	2	$m_{jj} > 350$	ggH-2j/$m_{jj} > 350$
VBF-1jet-tagged	VBF-1jet-tagged	—	—	qqH-rest
VBF-2jet-tagged-$m_{jj}[350,700]$	VBF-2jet-tagged	—	$p_T^{4\ell} < 200$, $p_T^{4\ell jj} < 25$, $350 < m_{jj} < 700$	qqH-2j/$m_{jj}[350,700]$
VBF-2jet-tagged-$m_{jj} > 700$	VBF-2jet-tagged	—	$p_T^{4\ell} < 200$, $p_T^{4\ell jj} < 25$, $m_{jj} > 700$	qqH-2j/$m_{jj} > 700$
VBF-3jet-tagged-$m_{jj} > 350$	VBF-2jet-tagged	—	$p_T^{4\ell} < 200$, $p_T^{4\ell jj} > 25$, $m_{jj} > 350$	qqH-3j/$m_{jj} > 350$
VBF-2jet-tagged-$p_T^{4\ell} > 200$	VBF-2jet-tagged	—	$p_T^{4\ell} > 200$, $m_{jj} > 350$	qqH-2j/$p_T > 200$
VBF-rest	VBF-2jet-tagged	—	$m_{jj} < 350$	qqH-rest
VH-hadronic-tagged-$m_{jj}[60,120]$	VH-hadronic-tagged	—	$60 < m_{jj} < 120$	qqH-2j/$m_{jj}[60,120]$
VH-rest	VH-hadronic-tagged	—	$m_{jj} < 60$ or $m_{jj} > 120$	qqH-rest
VH-leptonic-tagged-$p_T^{4\ell}[0,150]$	VH-leptonic-tagged	—	$p_T^{4\ell} < 150$	VH-lep/$p_T^H[0,150]$
VH-leptonic-tagged-$p_T^{4\ell} > 150$	VH-leptonic-tagged	—	$p_T^{4\ell} > 150$	VH-lep/$p_T^H > 150$
$t\bar{t}$H-leptonic-tagged	$t\bar{t}$H-leptonic-tagged	—	—	ttH
$t\bar{t}$H-hadronic-tagged	$t\bar{t}$H-hadronic-tagged	—	—	ttH

Eur. Phys. J. C 81 (2021) 488

Reconstructed Event categorization – Stage1.2

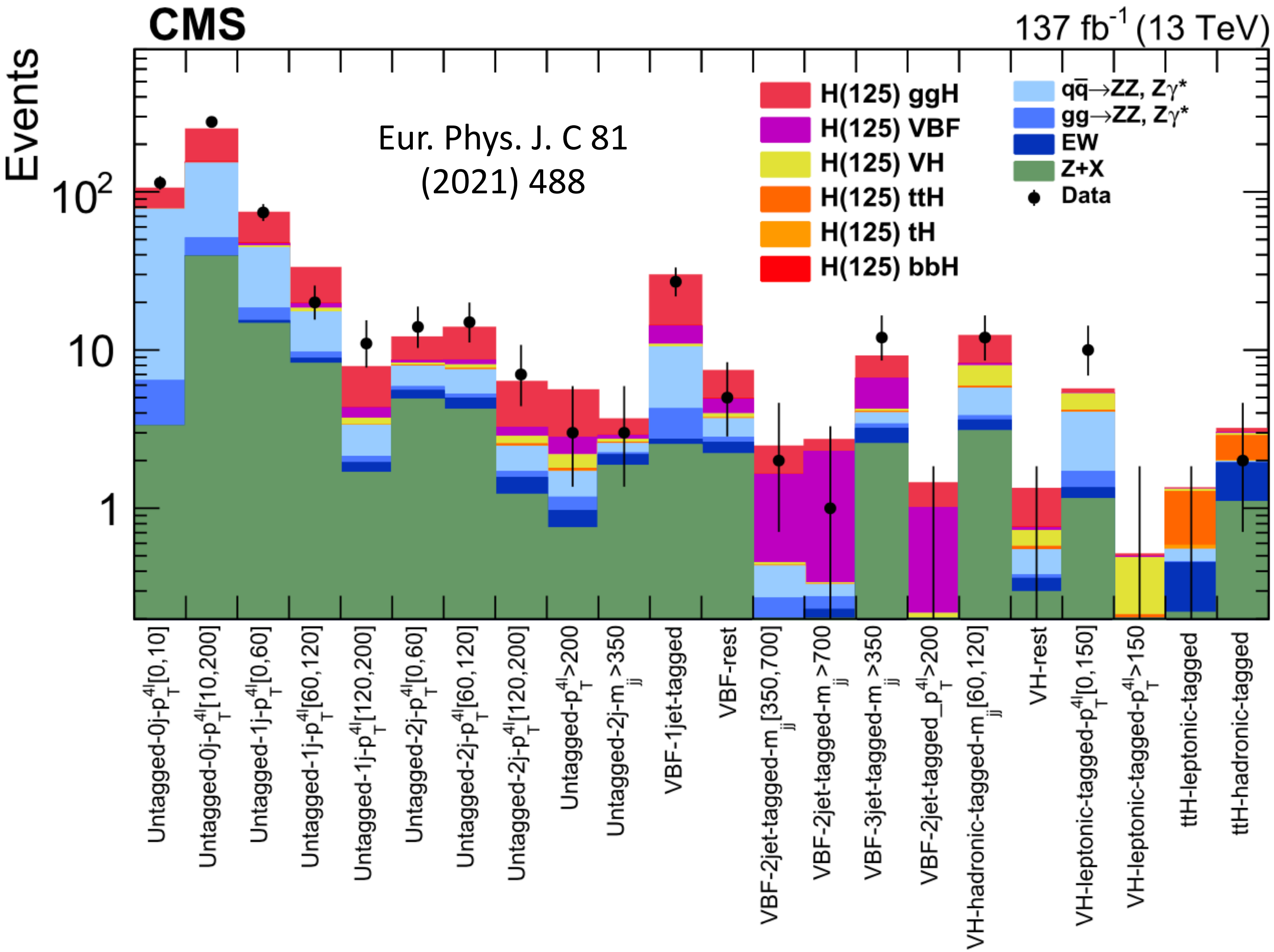

- Distributions of the expected and observed number of events for the reconstructed event categories in the mass region 105 < m4l < 140 GeV.
- The yields of the different H boson production mechanisms with mH = 125 GeV, and those of the ZZ and rare electroweak backgrounds are normalized to the SM expectations, while the Z+X background yield is normalized to the estimate from the data .

Background estimation

- Irreducible background
  - Production of ZZ via $q\bar{q}$ annihilation or gluon fusion
  - Estimated using simulation

Channel	4e	4μ	$2e2\mu$	4ℓ
$q\bar{q} \to ZZ$	333^{+57}_{-53}	622^{+31}_{-44}	815 ± 73	1770^{+98}_{-101}
$gg \to ZZ$	$75.1^{+14.3}_{-13.5}$	$116.6^{+11.7}_{-12.8}$	176.9 ± 23.0	$368.5^{+29.5}_{-29.6}$
$Z + X$	19.3 ± 7.2	50.8 ± 15.2	64.6 ± 15.6	134.7 ± 22.9
Sum of backgrounds	$428^{+59.2}_{55.2}$	$790^{+36.4}_{-48.3}$	1057 ± 78.1	$2274^{+104.9}_{-107.7}$
Signal ($m_H = 125$ GeV)	$19.6^{+3.3}_{-3.1}$	$40.8^{+2.5}_{-2.9}$	50.7 ± 5.6	$111.1^{+6.9}_{-7.0}$
Total expected	$447^{+59.3}_{55.2}$	$830^{+36.5}_{-48.4}$	1108 ± 78.3	$2385^{+105.1}_{-107.9}$
Observed	462	850	1130	2442

CMS PAS HIG-19-001

- Reducible background
  - Secondary leptons produced by heavy-flavor jets
  - Misidentified as leptons from decay of heavy-flavor hadron, in-flight decays of light mesons within jets, or (for electrons) decay of charged hadrons overlapping with π^0decays.
  - Two dependent methods used to estimated Z+X background: OS and SS
    - Fake rates calculated in Z+l control region
    - Z+X yields estimated in 2 orthogonal regions of Z+ll control region
    - Final estimate combination of 2 methods

Systematics Uncertainties

- The experimental uncertainties
  - mainly originating from the imperfect knowledge of the detector
  - depending on the year of data taking
  - Integrated luminosity
  - Lepton identification and reconstruction efficiency
- Theoretical uncertainties
  - accounting for the uncertainties in the modeling of the signal and background processes.
  - renormalization and factorization scale and choice of PDF set
- In combination of the three-year data, the theoretical uncertainties and experimental ones related to leptons or jets are treated as correlated while all other ones from experimental sources are taken as uncorrelated.

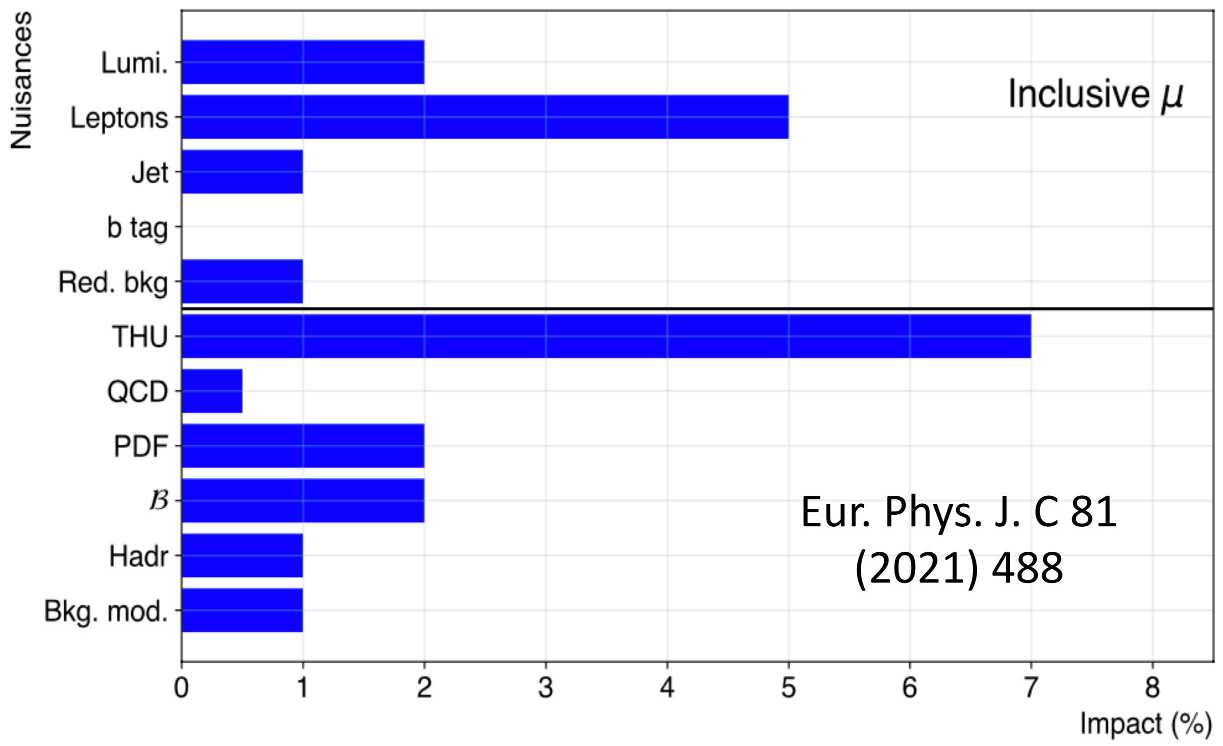

Eur. Phys. J. C 81 (2021) 488

Signal Strength – Production Models

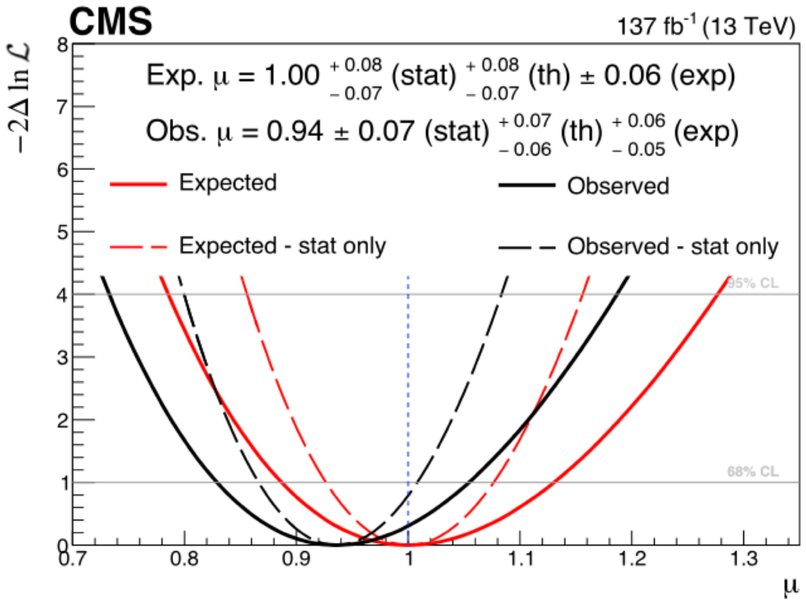

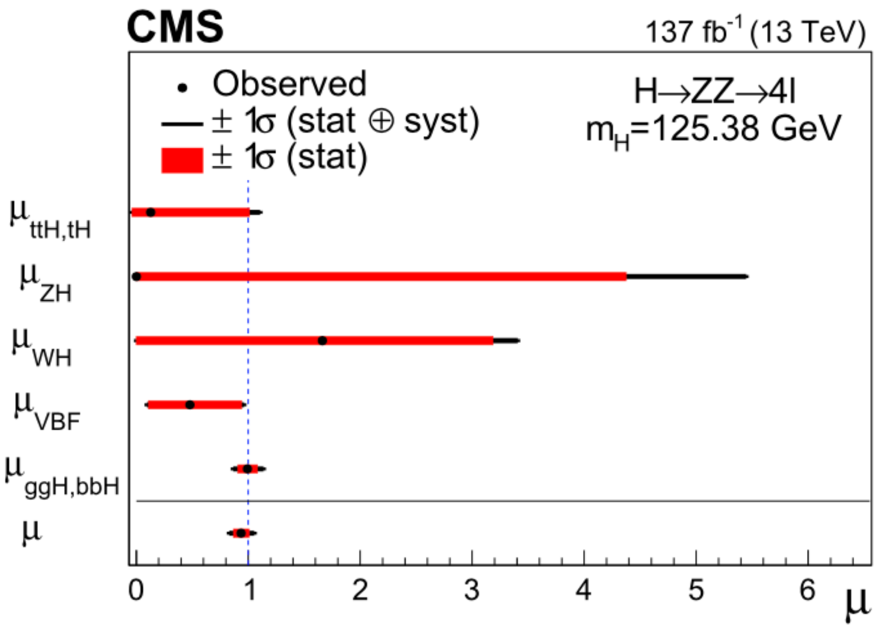

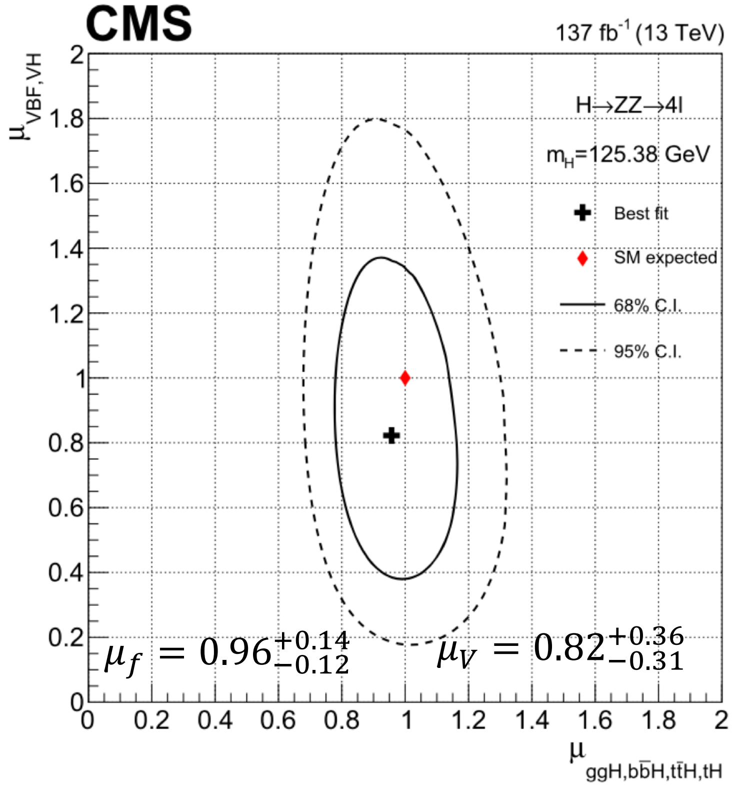

	Expected	Observed
$\mu_{t\bar{t}H,tH}$	$1.00^{+1.23}_{-0.77}$ (stat)$^{+0.51}_{-0.06}$ (syst)	$0.17^{+0.88}_{-0.17}$ (stat)$^{+0.42}_{-0.00}$ (syst)
μ_{WH}	$1.00^{+1.83}_{-1.00}$ (stat)$^{+0.75}_{-0.00}$ (syst)	$1.66^{+1.52}_{-1.66}$ (stat)$^{+0.85}_{-0.00}$ (syst)
μ_{ZH}	$1.00^{+4.79}_{-1.00}$ (stat)$^{+6.76}_{-0.00}$ (syst)	$0.00^{+4.38}_{-0.00}$ (stat)$^{+3.24}_{-0.00}$ (syst)
μ_{VBF}	$1.00^{+0.53}_{-0.44}$ (stat)$^{+0.18}_{-0.12}$ (syst)	$0.48^{+0.46}_{-0.37}$ (stat)$^{+0.14}_{-0.10}$ (syst)
$\mu_{ggH,b\bar{b}H}$	1.00 ± 0.10 (stat)$^{+0.12}_{-0.10}$ (syst)	0.99 ± 0.09 (stat)$^{+0.11}_{-0.09}$ (syst)
μ	$1.00^{+0.08}_{-0.07}$ (stat)$^{+0.10}_{-0.08}$ (syst)	0.94 ± 0.07 (stat)$^{+0.09}_{-0.08}$ (syst)

Eur. Phys. J. C 81 (2021) 488

- Perform multidimensional maximum likelihood fit to (m_{4l},KD) templates in 66channels (3×22)
- Total PDF is defined as: $\mathcal{L}_{2D}(m_{4\ell}, \mathcal{D}^{\text{kin}}_{\text{bkg}}) = \mathcal{L}(m_{4\ell})\mathcal{L}(\mathcal{D}^{\text{kin}}_{\text{bkg}}|m_{4\ell}).$

Simplified Template Cross Section

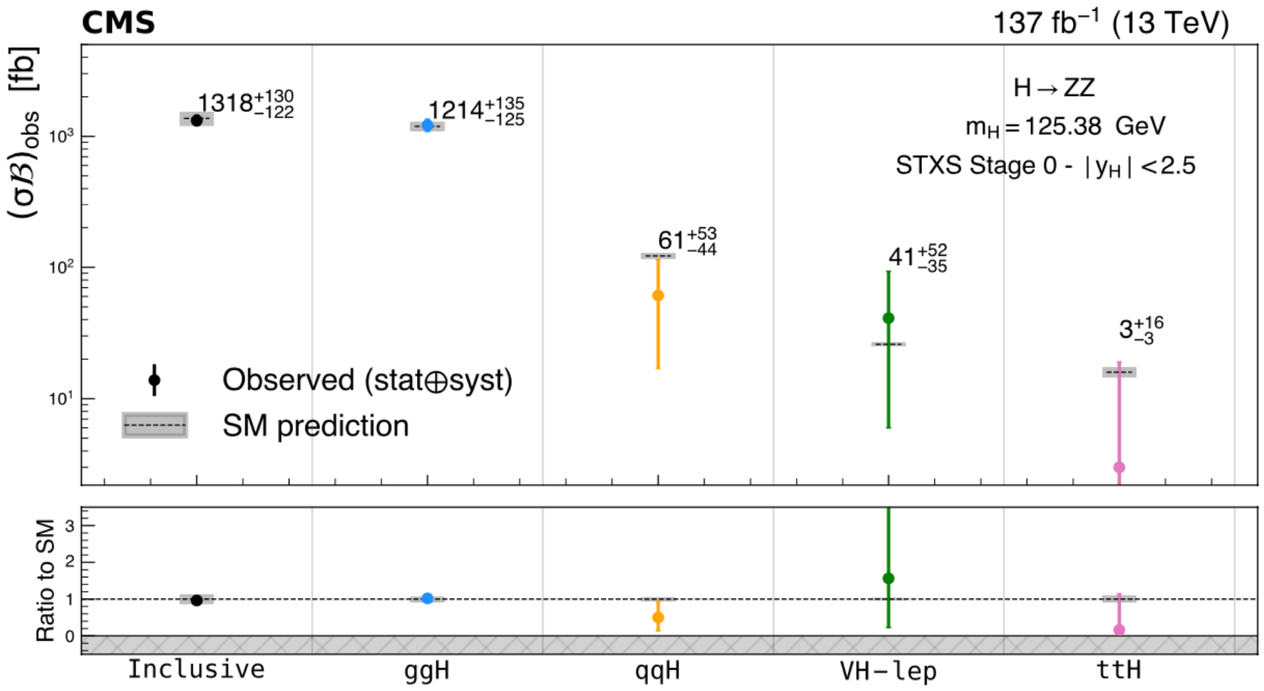

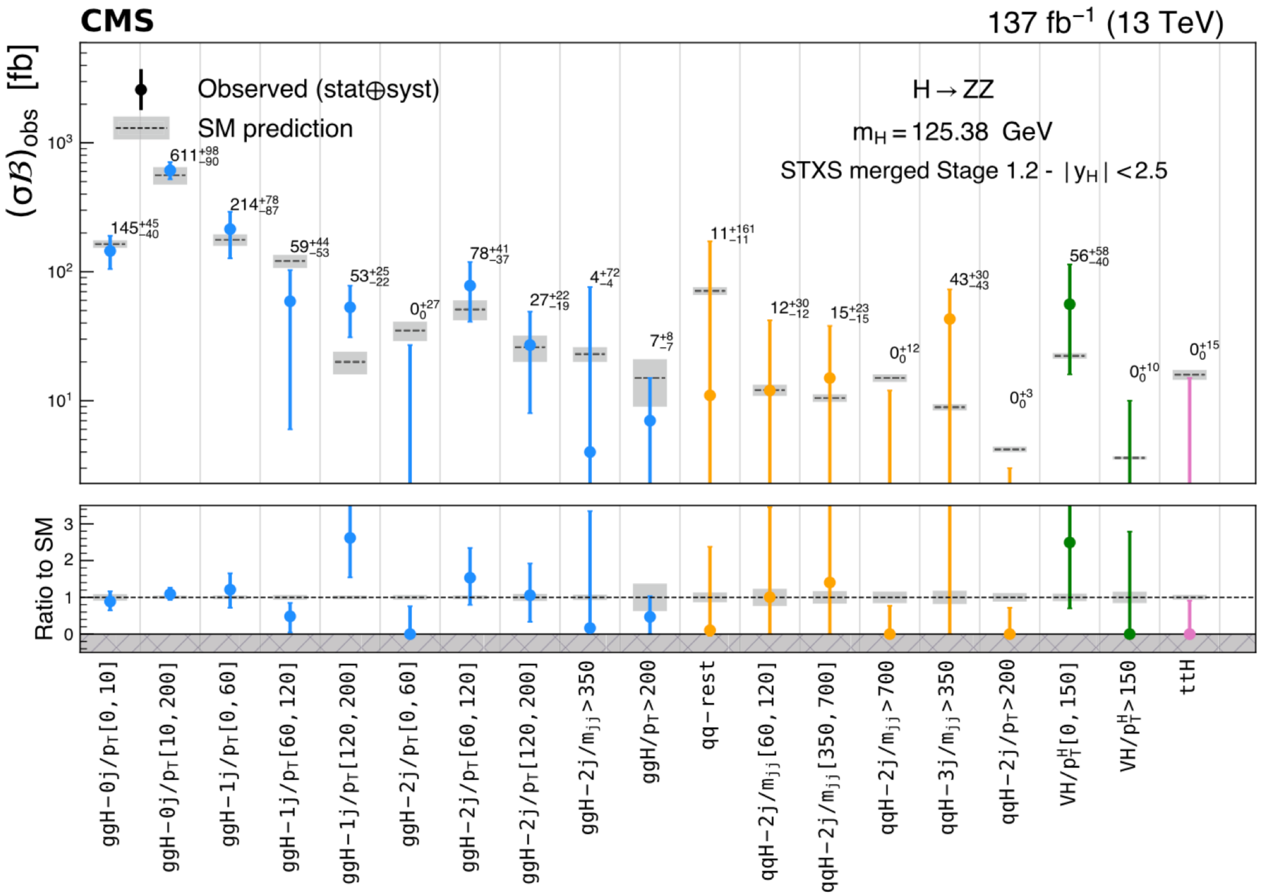

- The measured cross sections $(\sigma B)_{obs}$ and the SM predictions $(\sigma B)_{SM}$ for H → ZZ decay for the stage 0 STXS production bins and the inclusive measurement (left), the merged stage 1.2 STXS production bins (right) at m_H = 125.38 GeV

Eur. Phys. J. C 81 (2021) 488

Fiducial/Differential Cross Section

- This measurement has minimal dependence on the assumptions of the relative fraction or kinematic distributions of the separate production modes.

Requirements for the $H \to 4\ell$ fiducial phase space	
Lepton kinematics and isolation	
Leading lepton p_T	$p_T > 20$ GeV
Next-to-leading lepton p_T	$p_T > 10$ GeV
Additional electrons (muons) p_T	$p_T > 7(5)$ GeV
Pseudorapidity of electrons (muons)	$\lvert\eta\rvert < 2.5(2.4)$
Sum of scalar p_T of all stable particles within $\Delta R < 0.3$ from lepton	$< 0.35 \cdot p_T$
Event topology	
Existence of at least two same-flavor OS lepton pairs, where leptons satisfy criteria above	
Inv. mass of the Z_1 candidate	$40\,\text{GeV} < m_{Z_1} < 120\,\text{GeV}$
Inv. mass of the Z_2 candidate	$12\,\text{GeV} < m_{Z_2} < 120\,\text{GeV}$
Distance between selected four leptons	$\Delta R(\ell_i, \ell_j) > 0.02$ for any $i \neq j$
Inv. mass of any opposite sign lepton pair	$m_{\ell^+\ell'^-} > 4\,\text{GeV}$
Inv. mass of the selected four leptons	$105\,\text{GeV} < m_{4\ell} < 140\,\text{GeV}$

$$N_{\text{exp}}^{f,i}(m_{4\ell}) = N_{\text{fid}}^{f,i}(m_{4\ell}) + N_{\text{nonfid}}^{f,i}(m_{4\ell}) + N_{\text{nonres}}^{f,i}(m_{4\ell}) + N_{\text{bkg}}^{f,i}(m_{4\ell})$$
$$= \sum_j \epsilon_{i,j}^{f} \left(1 + f_{\text{nonfid}}^{f,i}\right) \sigma_{\text{fid}}^{f,j} \mathcal{L} \mathcal{P}_{\text{res}}(m_{4\ell})$$
$$+ N_{\text{nonres}}^{f,i} \mathcal{P}_{\text{nonres}}(m_{4\ell}) + N_{\text{bkg}}^{f,i} \mathcal{P}_{\text{bkg}}(m_{4\ell}).$$

Signal process	$\mathcal{A}_{\text{fid}}$	ϵ	f_{nonfid}	$(1 + f_{\text{nonfid}})\epsilon$
ggH (POWHEG)	0.402 ± 0.001	0.598 ± 0.002	0.054 ± 0.001	0.631 ± 0.002
VBF	0.445 ± 0.002	0.615 ± 0.002	0.043 ± 0.001	0.641 ± 0.003
WH	0.329 ± 0.002	0.604 ± 0.003	0.078 ± 0.002	0.651 ± 0.004
ZH	0.340 ± 0.003	0.613 ± 0.005	0.082 ± 0.004	0.663 ± 0.006
$t\bar{t}H$	0.315 ± 0.004	0.588 ± 0.007	0.181 ± 0.009	0.694 ± 0.010

The integrated fiducial cross section is measured to be

$$\sigma_{fid.} = 2.84^{+0.23}_{-0.22}(stat.)^{+0.26}_{-0.21}(syst.)fb$$

$$\sigma_{fid}^{SM} = 2.84 \pm 0.15 fb$$

Eur. Phys. J. C 81 (2021) 488

Fiducial/Differential Cross Section

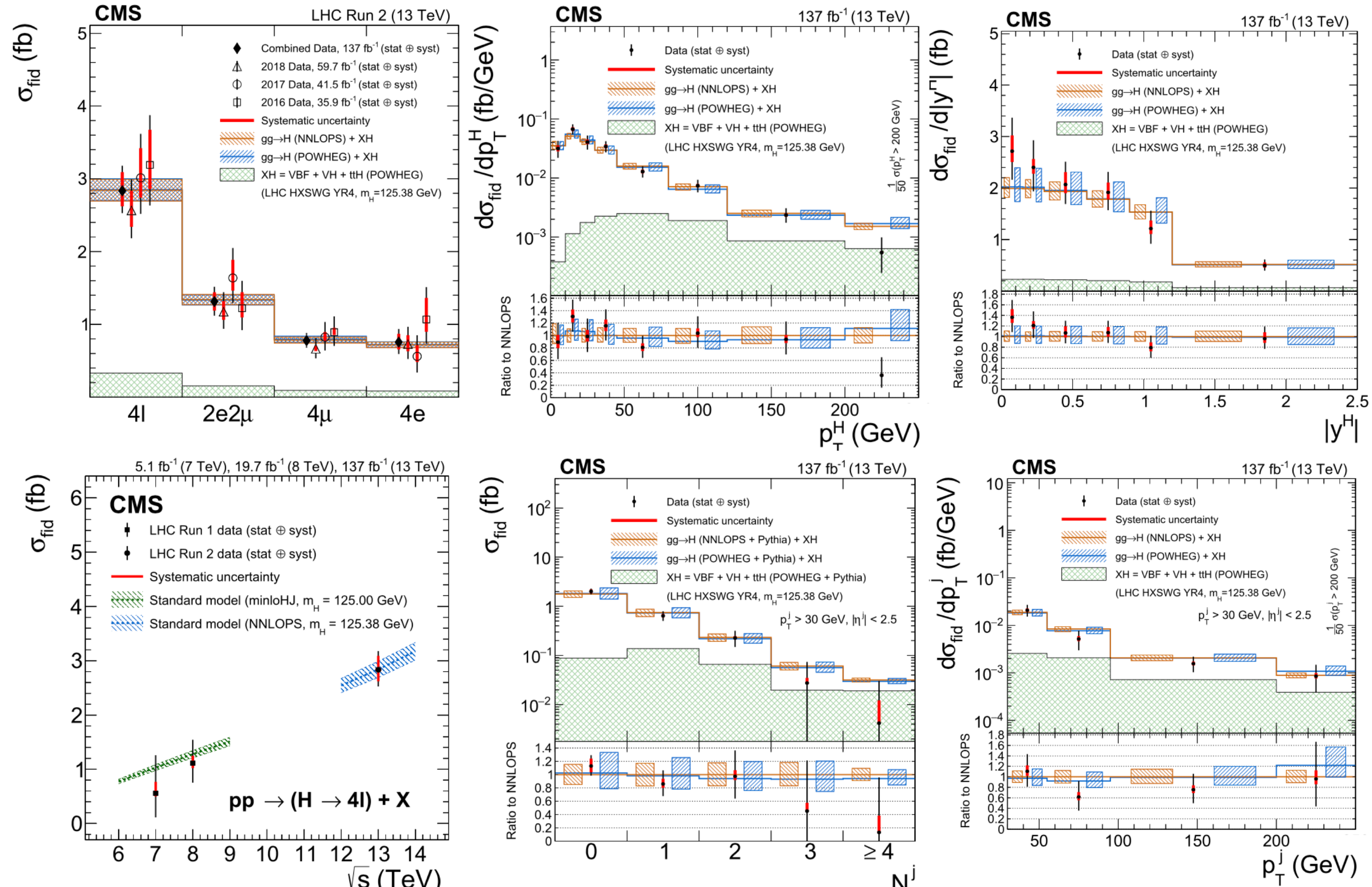

- The measured inclusive fiducial cross section in different final states and as a function of $\sqrt{s}$. (left)
- Differential cross sections as a function of the p_T and rapidity of the H boson, the number of associated jets, and the p_T of the leading associated jet are determined. (right)
- The sub-dominant component of the the signal (VBF + VH + $t\bar{t}$H) is denoted as XH.

Eur. Phys. J. C 81 (2021) 488

Summary

- Several measurements of Higgs boson production in four-lepton final state at $\sqrt{s} = 13 TeV$ are presented, using data sample corresponding to an integrated luminosity of 137.1 fb^{-1}.
  - The measured signal strength modifier is $\mu = 0.94 \pm 0.07(stat)^{+0.07}_{-0.06}(theo)^{+0.06}_{-0.05}(exp)$.
  - A new set of cross section measurements in mutually exclusive categories targeted to identify production mechanisms and kinematical features of the events is presented.
  - Differential cross sections as a function of the transverse momentum and rapidity of the Higgs boson, the number of associated jets, and the transverse momentum of the leading associated jet are measured.
- All results are consistent, within their uncertainties, with the expectations for the Standard Model H boson.

Backup

Distribution of m_{4l} of Run-2 data

Eur. Phys. J. C 81 (2021) 488

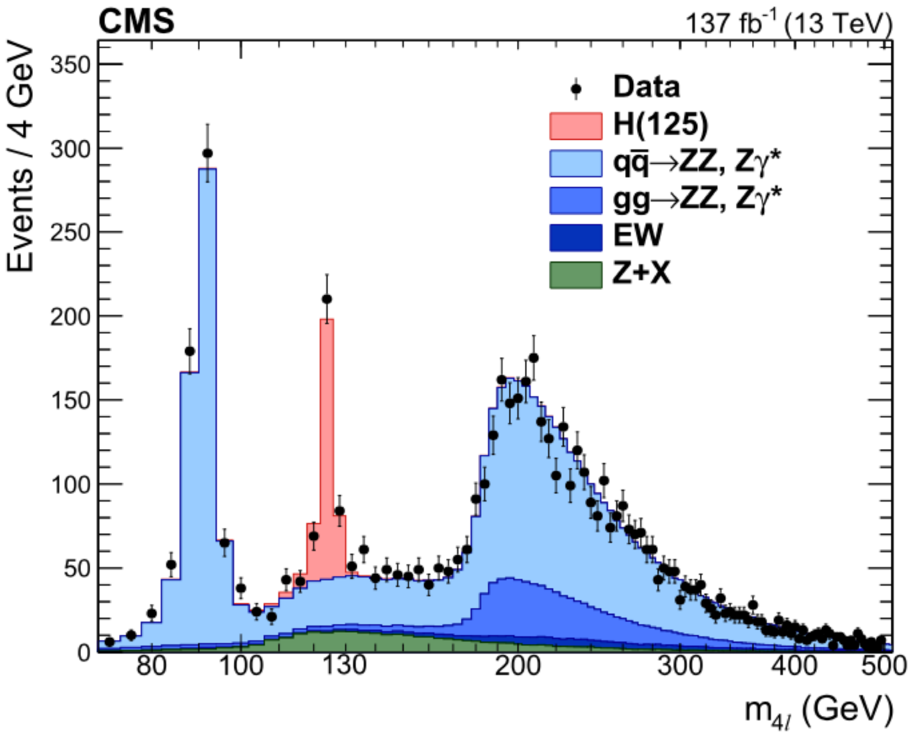

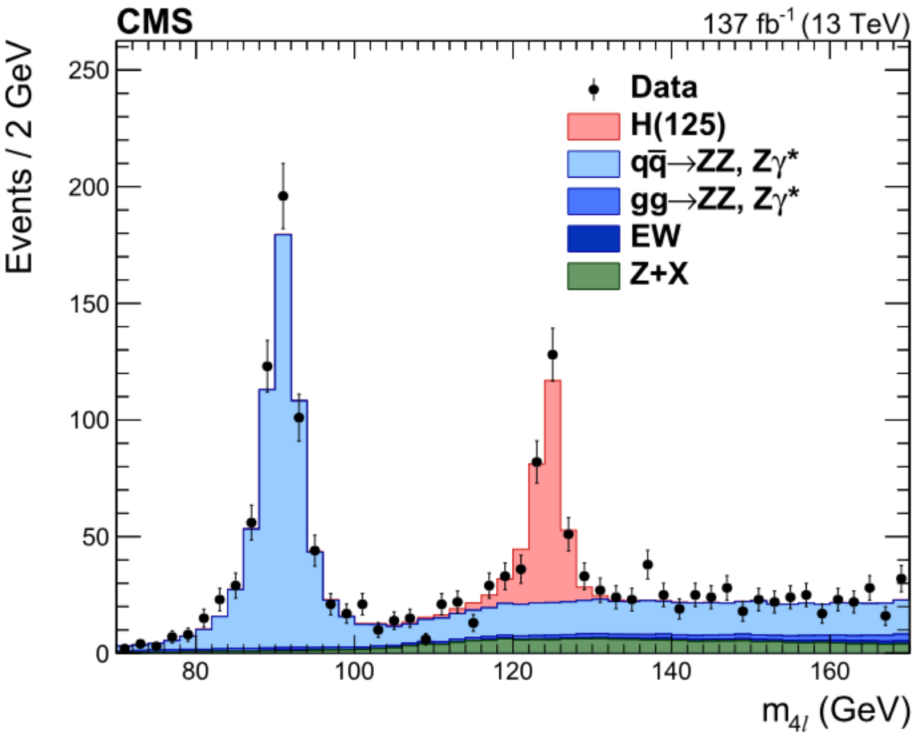

Distribution of m_{4l} VS kinematic discriminants

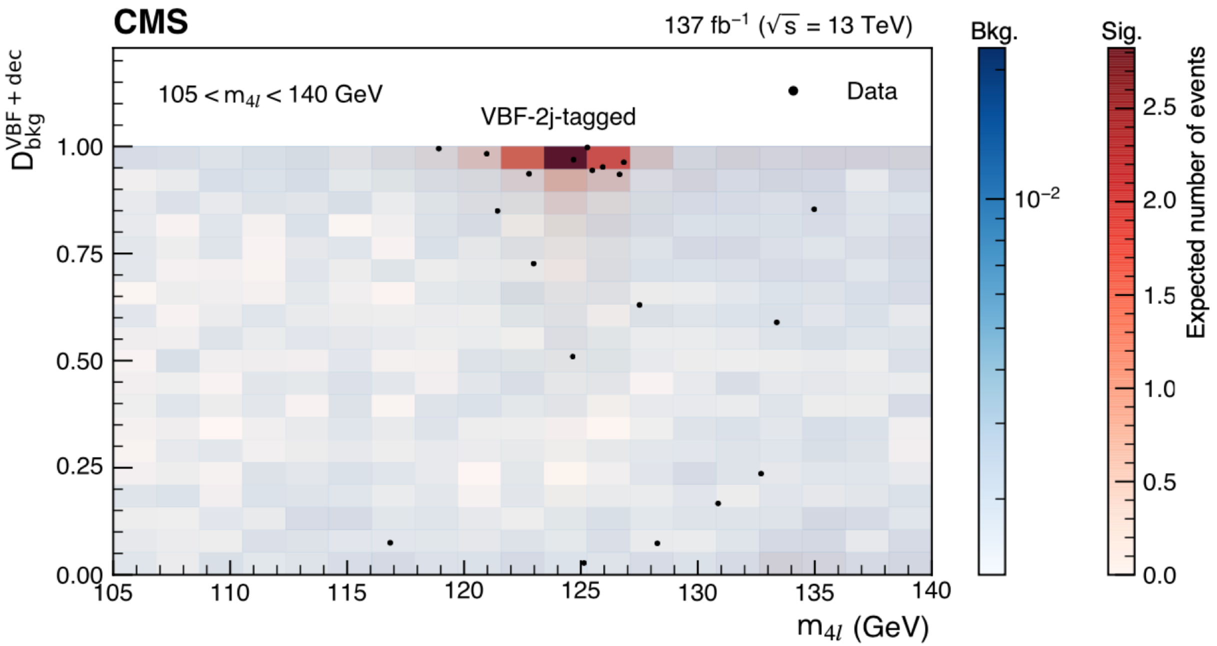

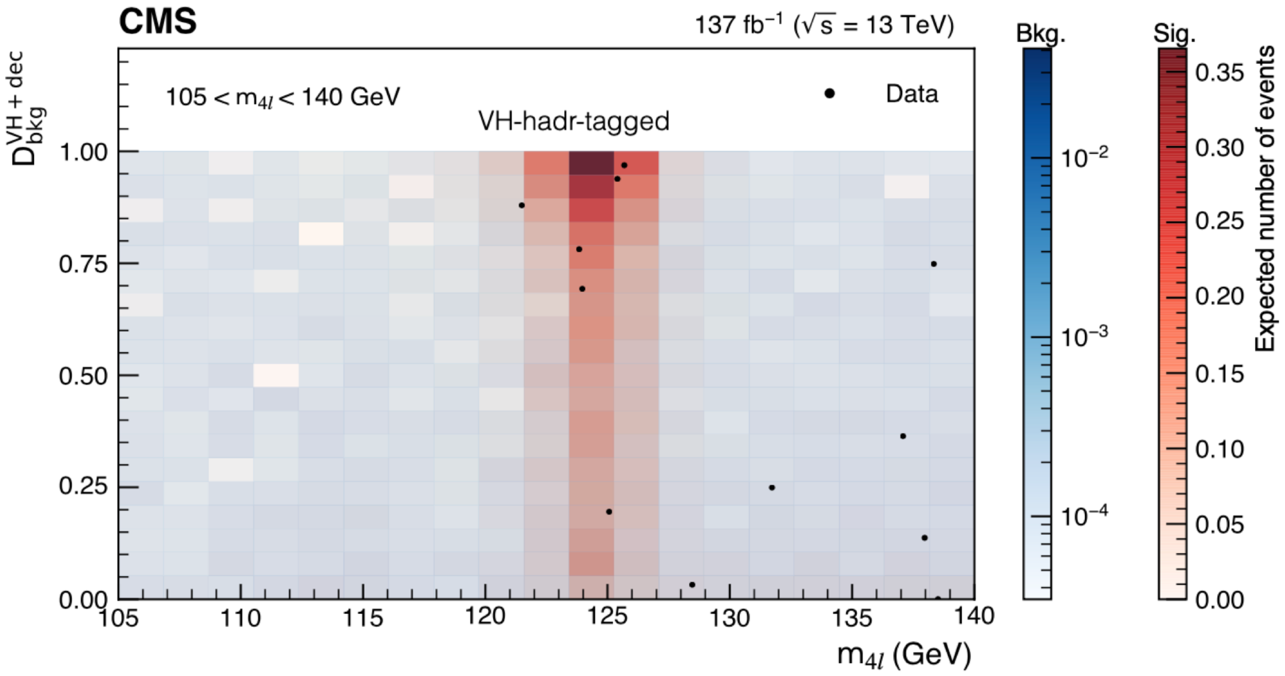

- Distribution of three different kinematic discriminants versus m_{4l} : $D_{bkg}^{VBF+dec}$ (left) and D_{bkg}^{VH+dec} (right) shown in the mass region 105 < *m* < 140GeV.
- The blue scale represents the expected total number of ZZ, rare electroweak, and Z+X background events.
- The red scale represents the number of expected SM H boson signal events for m_H = 125 GeV.
- The points show the data from the categories listed in the legend.

Eur. Phys. J. C 81 (2021) 488

Distribution of Z_1 and Z_2

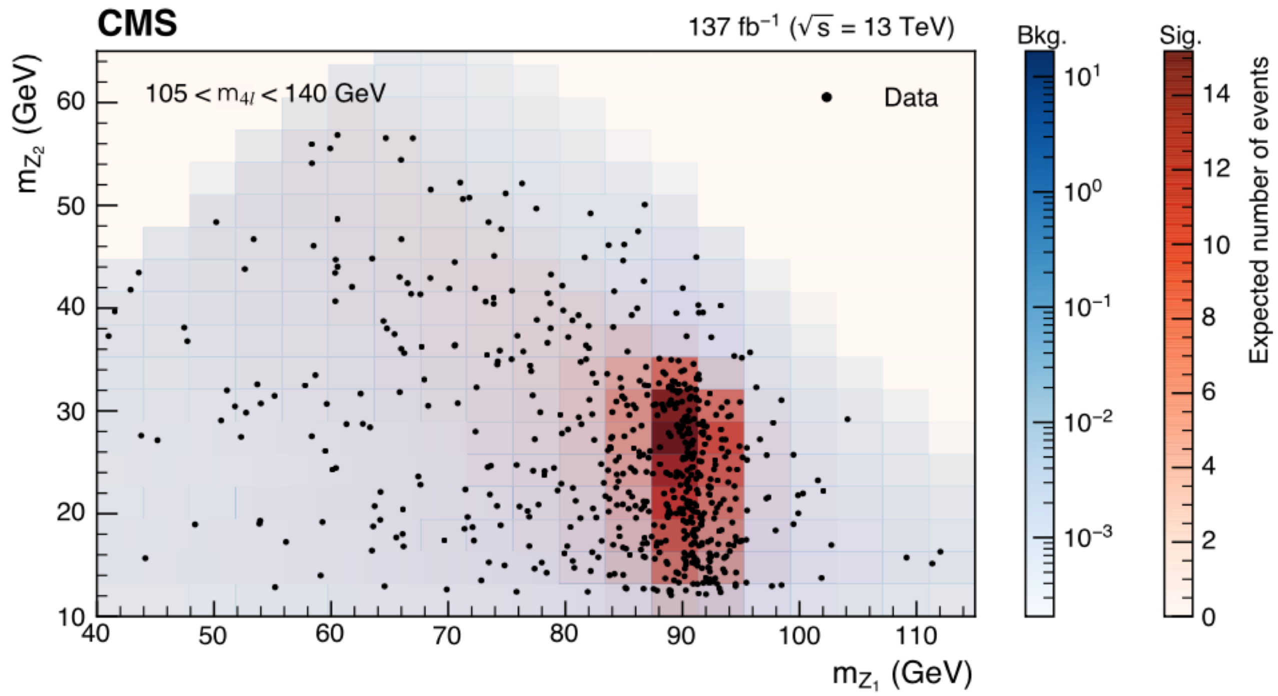

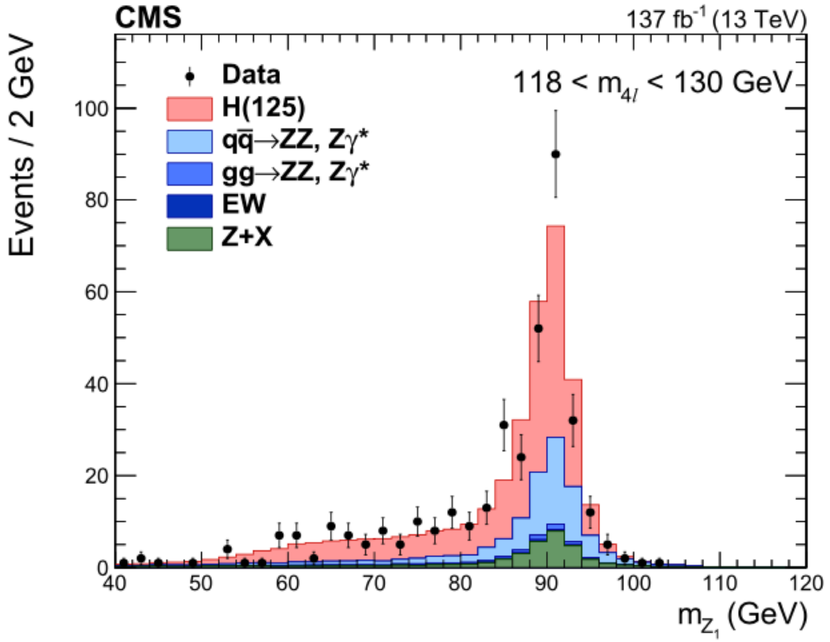

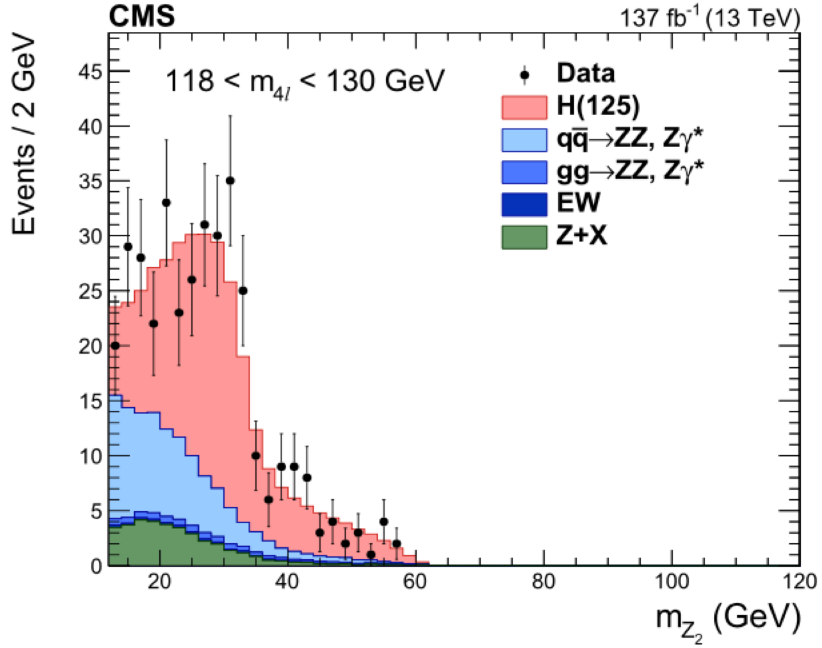

Eur. Phys. J. C 81 (2021) 488

Distribution of discriminant

Eur. Phys. J. C 81 (2021) 488

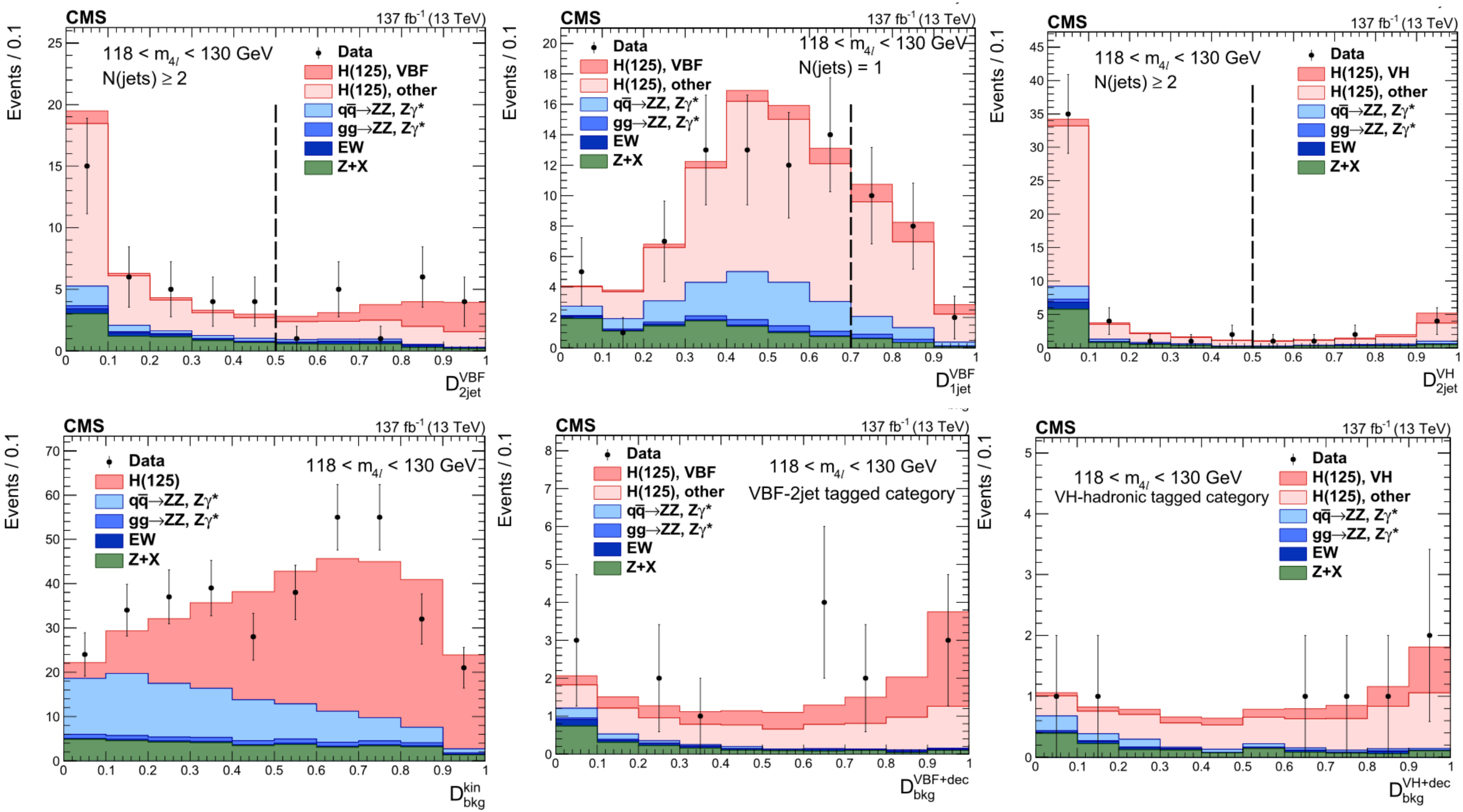

Category discriminant

Kinematic discriminant

Expected Yields

Eur. Phys. J. C 81 (2021) 488

Reconstructed event	Signal							Background				Expected		Observed
category	ggH	VBF	WH	ZH	$t\bar{t}H$	$b\bar{b}H$	tH	$q\bar{q} \to ZZ$	$gg \to ZZ$	EW	Z+X	signal	total	
Untagged-0j-$p_T^{4\ell}[0,10]$	27.7	0.09	0.03	0.03	0.00	0.15	0.00	71.5	3.06	0.01	3.21	27.9±0.1	106±0	114
Untagged-0j-$p_T^{4\ell}[10,200]$	96.2	1.69	0.60	0.77	0.01	1.01	0.00	98.1	11.6	0.35	37.8	100±0	248±1	278
Untagged-1j-$p_T^{4\ell}[0,60]$	26.8	1.51	0.56	0.48	0.01	0.45	0.01	25.3	3.02	0.64	14.2	29.8±0.1	72.9±0.4	74
Untagged-1j-$p_T^{4\ell}[60,120]$	13.5	1.31	0.51	0.41	0.02	0.11	0.01	7.81	0.82	0.62	7.95	15.9±0.1	33.1±0.3	20
Untagged-1j-$p_T^{4\ell}[120,200]$	3.51	0.60	0.17	0.17	0.01	0.02	0.00	1.15	0.19	0.25	1.63	4.48±0.05	7.69±0.16	11
Untagged-2j-$p_T^{4\ell}[0,60]$	3.45	0.29	0.15	0.14	0.08	0.09	0.02	2.14	0.32	0.63	4.75	4.20±0.06	12.1±0.2	14
Untagged-2j-$p_T^{4\ell}[60,120]$	5.26	0.56	0.24	0.19	0.12	0.04	0.03	2.19	0.30	0.72	4.14	6.43±0.06	13.8±0.2	15
Untagged-2j-$p_T^{4\ell}[120,200]$	3.07	0.40	0.16	0.13	0.07	0.01	0.02	0.75	0.14	0.34	1.19	3.86±0.05	6.28±0.14	7
Untagged-$p_T^{4\ell} > 200$	2.79	0.62	0.21	0.17	0.07	0.01	0.02	0.43	0.21	0.21	0.73	3.89±0.04	5.47±0.11	3
Untagged-2j-$m_{jj} > 350$	0.77	0.16	0.06	0.04	0.05	0.01	0.01	0.34	0.06	0.31	1.71	1.12±0.02	3.54±0.14	3
VBF-1jet-tagged	15.5	3.29	0.22	0.16	0.00	0.13	0.01	6.85	1.53	0.20	2.44	19.3±0.1	30.3±0.2	27
VBF-2jet-tagged-$m_{jj}[350,700]$	0.83	1.19	0.01	0.01	0.00	0.01	0.00	0.19	0.07	0.11	0.14	2.05±0.03	2.55±0.05	2
VBF-2jet-tagged-$m_{jj} > 700$	0.43	1.96	0.00	0.00	0.00	0.00	0.00	0.07	0.05	0.12	0.03	2.40±0.02	2.67±0.03	1
VBF-3jet-tagged-$m_{jj} > 350$	2.52	2.35	0.06	0.06	0.03	0.03	0.05	0.62	0.21	0.64	2.43	5.11±0.05	9.01±0.17	12
VBF-2jet-tagged-$p_T^{4\ell} > 200$	0.44	0.79	0.01	0.01	0.01	0.00	0.01	0.03	0.03	0.04	0.06	1.26±0.02	1.42±0.03	0
VBF-rest	2.48	0.94	0.13	0.09	0.04	0.04	0.01	0.98	0.20	0.39	2.18	3.74±0.05	7.49±0.17	5
VH-hadronic-tagged-$m_{jj}[60,120]$	4.11	0.25	1.09	0.96	0.13	0.06	0.02	1.69	0.22	0.52	2.93	6.62±0.06	12.0±0.2	12
VH-rest	0.57	0.03	0.09	0.06	0.03	0.01	0.00	0.16	0.02	0.06	0.33	0.79±0.02	1.36±0.06	0
VH-leptonic-tagged-$p_T^{4\ell}[0,150]$	0.33	0.04	0.85	0.26	0.10	0.03	0.03	2.16	0.36	0.19	1.11	1.64±0.02	5.47±0.13	10
VH-leptonic-tagged-$p_T^{4\ell} > 150$	0.02	0.01	0.21	0.06	0.04	0.00	0.01	0.05	0.01	0.03	0.08	0.35±0.01	0.52±0.03	0
$t\bar{t}H$-leptonic-tagged	0.02	0.01	0.02	0.02	0.68	0.00	0.03	0.08	0.01	0.23	0.21	0.79±0.01	1.32±0.07	0
$t\bar{t}H$-hadronic-tagged	0.18	0.05	0.03	0.05	0.86	0.01	0.03	0.03	0.01	0.82	1.06	1.22±0.01	3.15±0.14	2

The impact of the dominant systematic uncertainties

Eur. Phys. J. C 81 (2021) 488

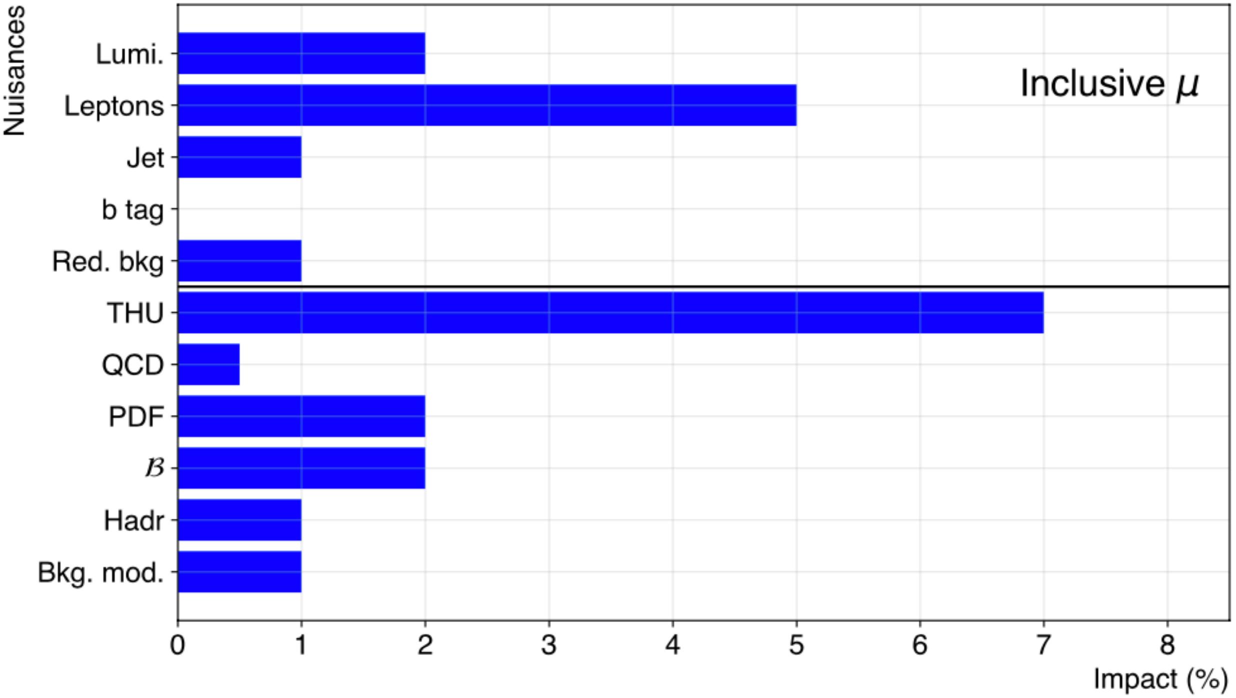

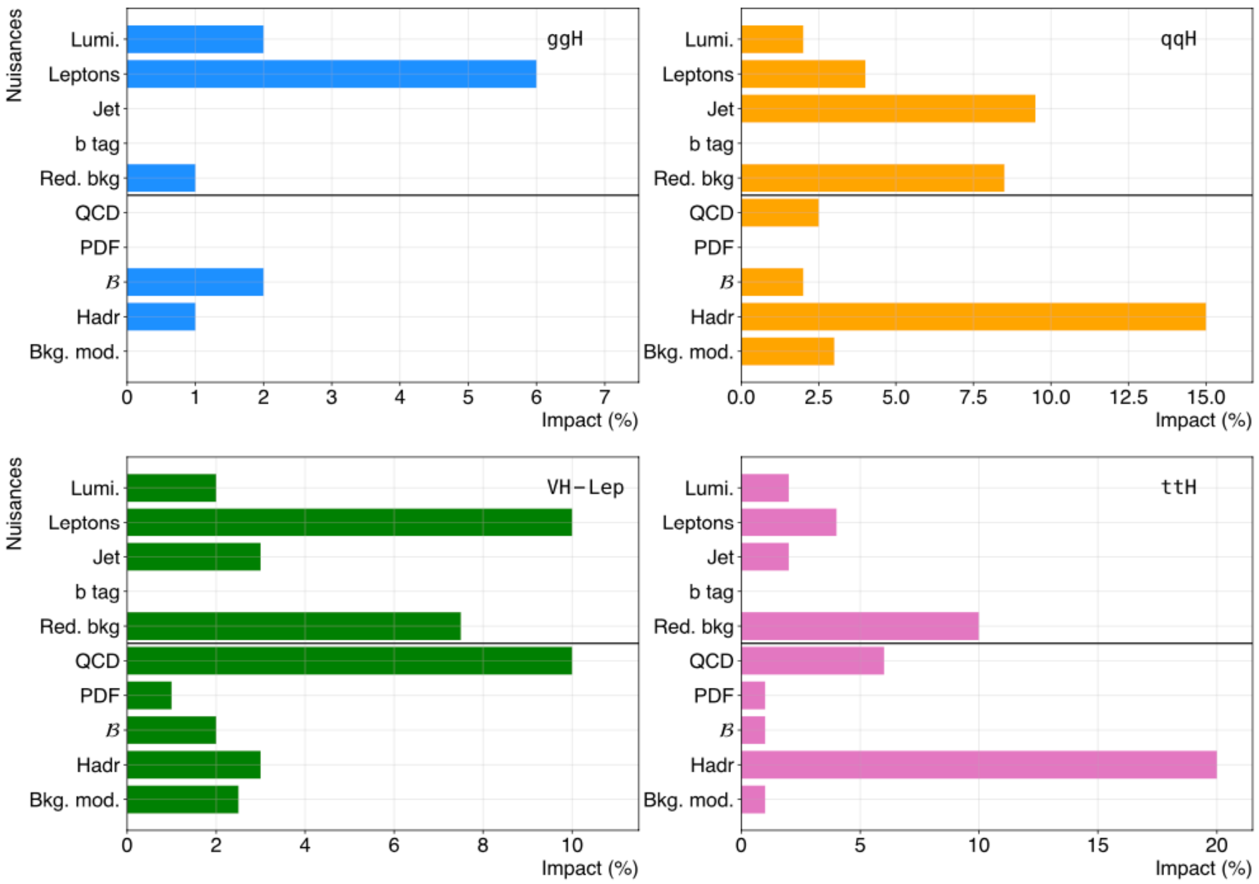

Event categorization – Stage0

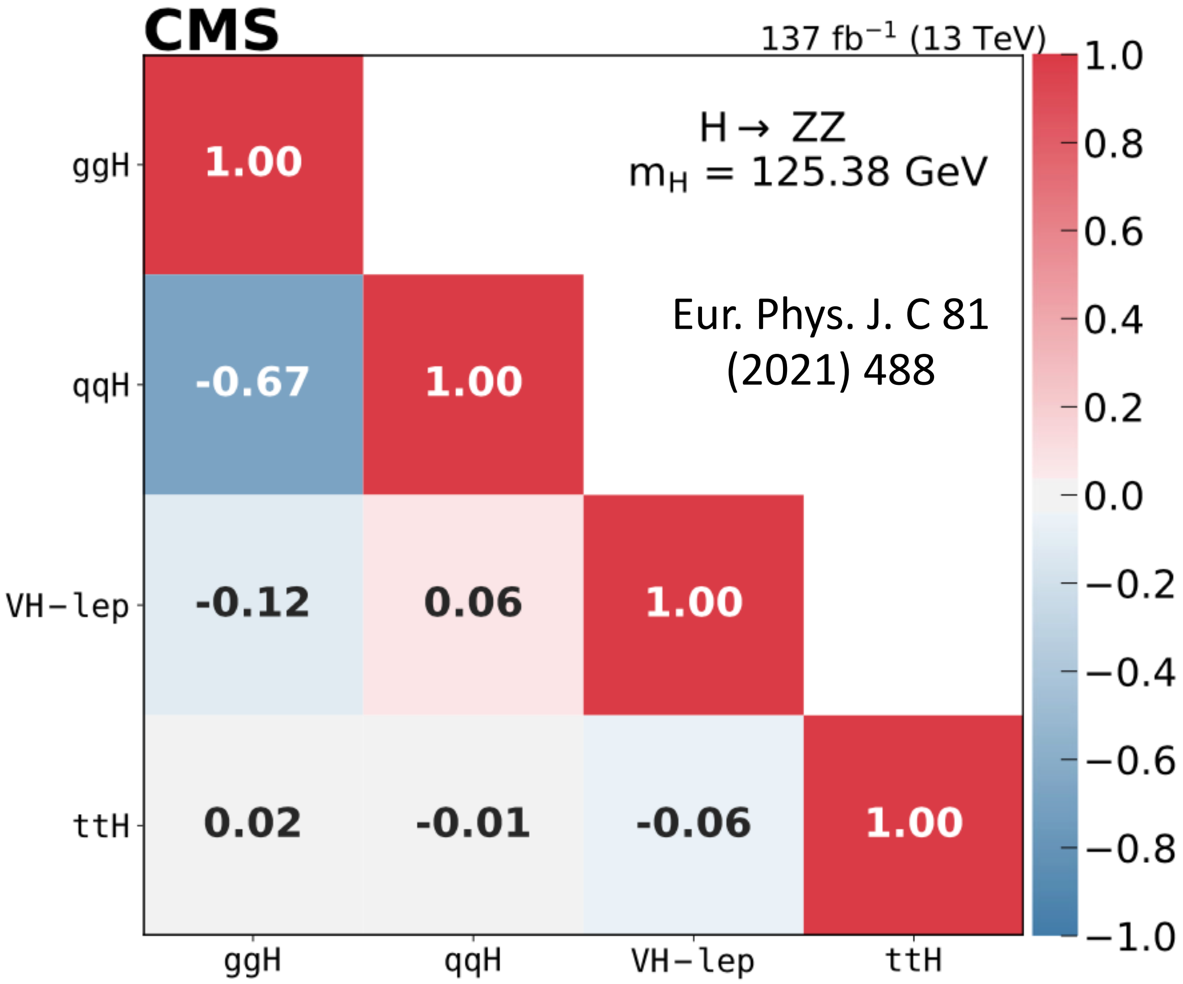

- Correlation matrices between the measured cross sections for the stage 0 for H → ZZ decay

Event categorization – Stage1.2

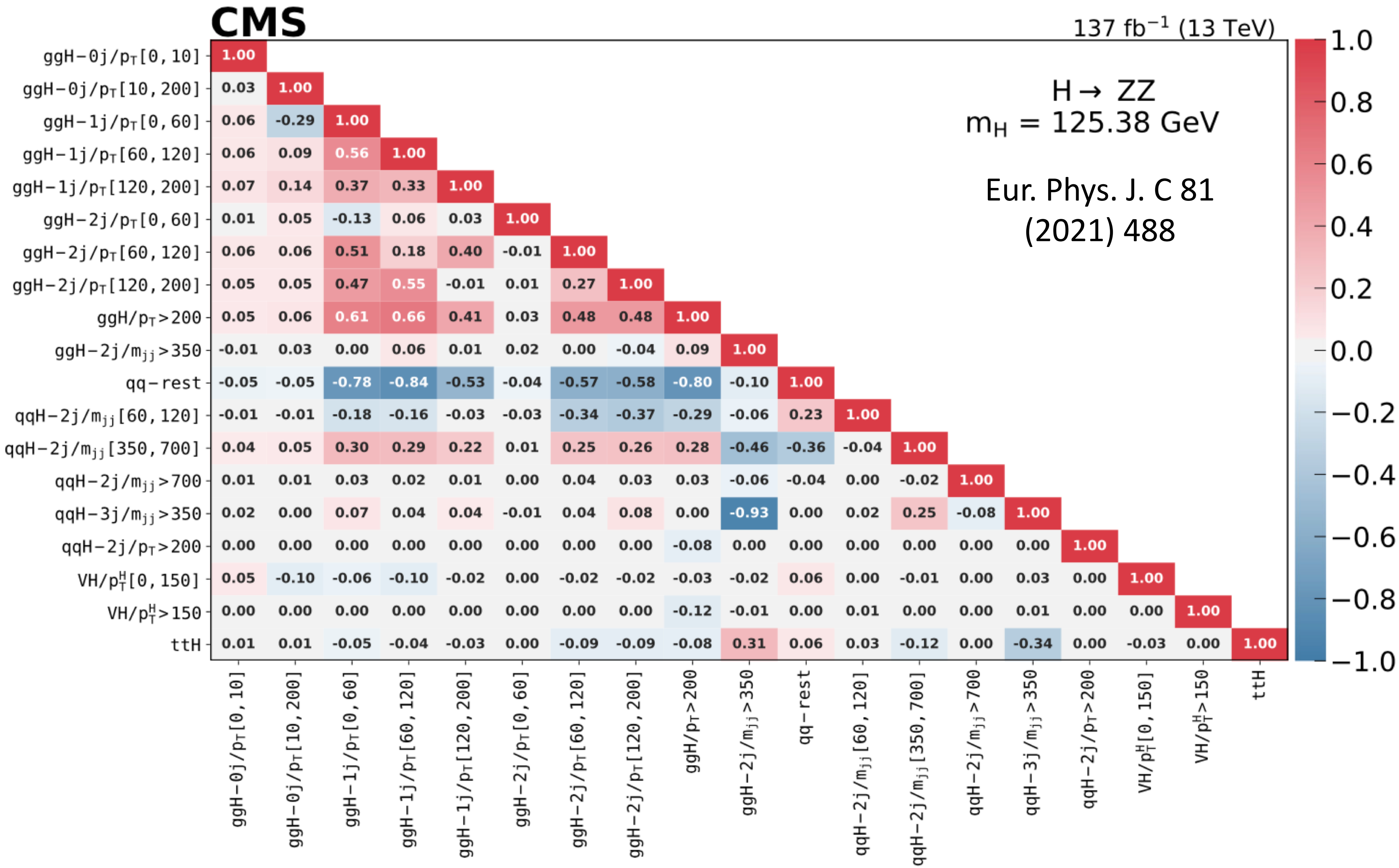

- Correlation matrices between the measured cross sections for the merged stage 1.2 for H → ZZ decay